

## Prediction of self-heating measurements under proportional and non-proportional multiaxial cyclic loadings

Martin Poncelet<sup>a,\*</sup>, Cédric Doudard<sup>b</sup>, Sylvain Calloch<sup>b</sup>, François Hild<sup>a</sup>,  
Bastien Weber<sup>c</sup>, André Galtier<sup>c</sup>

<sup>a</sup> LMT-Cachan, ENS de Cachan, CNRS–UMR 8535, université Paris 6, 61, avenue du Président-Wilson, 94235 Cachan cedex, France

<sup>b</sup> Laboratoire de mécanique des structures navales, ENSIETA, 2, rue François-Verny, 29806 Brest cedex 9, France

<sup>c</sup> ARCELOR Research, voie romaine, BP 30320, 57283 Maizières-lès-Metz cedex, France

Received 4 October 2006; accepted after revision 9 January 2007

Available online 12 February 2007

Presented by Évariste Sanchez-Palencia

---

### Abstract

Self-heating measurements under cyclic loadings allow for fast estimations of fatigue properties. These tests are performed under tension–torsion loadings on a medium-carbon steel and a model accounting for heterogeneities is proposed to analyse heat transfer results. Both proportional and non-proportional loading paths are predicted. **To cite this article:** M. Poncelet et al., *C. R. Mecanique 335 (2007)*.

© 2007 Académie des sciences. Published by Elsevier Masson SAS. All rights reserved.

### Résumé

**Prévision d'essais d'auto-échauffement sous chargements multiaxiaux hétérogènes.** Les essais d'auto-échauffement permettent une estimation rapide des caractéristiques de fatigue. Ils sont réalisés ici sur un acier C45 sous chargements de traction–torsion. Un modèle prenant en compte l'hétérogénéité de la dissipation est proposé. Il permet de rendre compte des mesures thermiques sous trajets proportionnels et non-proportionnels. **Pour citer cet article :** M. Poncelet et al., *C. R. Mecanique 335 (2007)*.

© 2007 Académie des sciences. Published by Elsevier Masson SAS. All rights reserved.

**Keywords:** Fatigue; Microplasticity; Poisson point process; Heterogeneous stress; Dissipation

**Mots-clés :** Fatigue ; Microplasticité ; Processus ponctuel de Poisson ; Contraintes hétérogènes ; Dissipation

---

### Version française abrégée

Les essais d'auto-échauffement permettent une estimation rapide des caractéristiques de fatigue pour certains métaux et alliages [2], et sont donc une alternative intéressante aux longs essais de fatigue multiaxiale traditionnels. Une modélisation probabiliste de l'apparition de la microplasticité permet de relier quantitativement essais d'auto-

---

\* Corresponding author.

E-mail addresses: poncelet@lmt.ens-cachan.fr (M. Poncelet), cedric.doudard@ensieta.fr (C. Doudard), sylvain.calloch@ensieta.fr (S. Calloch), hild@lmt.ens-cachan.fr (F. Hild), weber@arcelor.com (B. Weber), galtier@arcelor.com (A. Galtier).

échauffement et dispersion en fatigue. La probabilité de trouver  $k$  ‘sites’ (amas de grains siège de déformations plastiques) est piloté par un processus ponctuel de Poisson (1) d’intensité dépendant d’une contrainte équivalente d’activation  $\Sigma_a$  (2). L’énergie dissipée par cycle d’un site  $D_{\text{inc}}$  est calculée grâce à une loi de localisation (3) ainsi qu’une contrainte équivalente de plasticité de von Mises et une loi d’écrouissage cinématique linéaire. La dissipation totale est obtenue par intégration sur l’ensemble de la population de grains actifs (5). Sous hypothèse d’homogénéité de la température, celle-ci est obtenue par introduction dans l’équation de la chaleur (7) de la dissipation globale de la zone utile  $\Delta$  donnée par (6). Moyennant l’introduction d’un facteur d’hétérogénéité  $G_{m+2}$ ,  $\Delta$  s’exprime en fonction d’une contrainte effective  $\Sigma_{\text{eff diss}}$  (8). Ce facteur se calcule en (9) pour des chargements proportionnels ou numériquement pour des trajets non-proportionnels. Dans le cas de chargements de traction–torsion, l’hypothèse d’homogénéité est vérifiée et le facteur  $G_{m+2}$  est donné par (16) dans le cas proportionnel. Les résultats d’essais permettent de valider la contrainte effective proposée (Fig. 2(b)). On montre qu’on est capable de prévoir les courbes d’auto-échauffement sous chargement proportionnel ou non-proportionnel à partir d’un seul résultat pour l’identification des paramètres.

## 1. Introduction

For several years, different methods for the rapid estimation of mean fatigue limit based on temperature measurements have been developed. These tests consist in measuring the change of the specimen temperature under (usually) uniaxial cyclic loadings with thermocouples [1,2] or thermography [3,4]. The amplitude of loading is step-wise constant and risen once the temperature is stabilised. The steady-state temperature is plotted as a function of the loading amplitude as shown in Fig. 2. For some materials (e.g., steel or cast iron), a first part of the curve shows virtually no change in temperature, whereas in the second part the temperature rises significantly with the stress amplitude. A correlation between the mean fatigue limit and the stress level leading to the temperature increase has been empirically proposed [3,4,2]. Currently, models [5,6] based on microplasticity are developed to describe this result. To take into account the progressive onset of microplasticity two approaches are proposed. In the first one [5], the authors consider that the volume fraction of microplastic inclusion depends on the stress amplitude. In the second one [2], a probabilistic approach is used. The last model enables one to relate the fatigue behaviour with temperature measurements.

The investigation of multiaxial fatigue needs time-consuming experimental databases (e.g., stair-case tests for each loading direction). Applying temperature measurements to multiaxial fatigue is thus very interesting as shown with biaxial loadings [7]. However, it is seldom performed. It is proposed to carry out and analyse a more common type of loading such as tension–torsion. First, a probabilistic two-scale model is extended to multiaxial heterogeneous loadings. Then it is applied and finally validated with proportional and non-proportional loading results.

## 2. Modeling

### 2.1. Model basis

Gradual rise of heat (and thus temperature) is supposed to be a consequence of a random onset of microplasticity, which has been observed on low carbon steel [8]. The distribution of active grains (later called ‘sites’) in relation to their surrounding explains the ‘probabilistic’ feature, which is modeled by a Poisson Point Process. The probability of finding  $k$  sites in a domain  $\Omega$  of volume  $V$  reads

$$P_k(V) = \frac{(\lambda V)^k}{k!} \exp(-\lambda V) \quad (1)$$

where  $\lambda V$  is the mean number of sites under a given load amplitude and  $\lambda$  the ‘intensity’ of the Poisson Point Process, depending on an equivalent stress  $\Sigma_a$  (later called ‘Equivalent Activation Stress’) of the load amplitude and two material parameters  $m$  and  $V_0 S_0^m$

$$\lambda = \frac{1}{V_0} \left( \frac{\Sigma_a}{S_0} \right)^m \quad (2)$$

where  $\Sigma_a$  is supposed to be equal to von Mises equivalent stress amplitude  $\Sigma_0^{\text{eq}}$ . Experimental validation was performed for a Dual Phase steel [7]. The stress tensor in the plastic inclusion  $\sigma$  is related to the macroscopic stress tensor  $\Sigma$  and the corresponding strain tensor  $\epsilon^P$  by [9]

$$\sigma = \Sigma - 2\mu(1-\beta)\epsilon^P \quad (3)$$

where  $\mu$  denotes the shear modulus and  $\beta$  a constant related to the Poisson's ratio of the material.

The magnitude of the intrinsic dissipated energy  $D_{\text{inc}}(\Sigma_0^{\text{eq}}, \sigma_y)$  in a site over a loading cycle is calculated for a given value of the yield stress  $\sigma_y$  and a von Mises equivalent stress amplitude  $\Sigma_0^{\text{eq}}$ . A von Mises equivalent stress for the plasticity criterion associated with a linear kinematic hardening is assumed. For a uniform proportional loading,  $D_{\text{inc}}(\Sigma_0^{\text{eq}}, \sigma_y)$  is given by

$$D_{\text{inc}}^{\text{prop}}(\Sigma_0^{\text{eq}}, \sigma_y) = \frac{4\sigma_y^u}{h} \langle \Sigma_0^{\text{eq}} - \sigma_y^u \rangle \quad (4)$$

where  $h$  is the hardening modulus. The total dissipated energy is then obtained by integration over the whole population of sites [6]

$$D(\Sigma_0^{\text{eq}}) = \int_0^{\Sigma_0^{\text{eq}}} D_{\text{inc}}(\Sigma_0^{\text{eq}}, \sigma) \frac{d\lambda}{d\sigma} d\sigma \quad (5)$$

For a heterogeneous stress field over a domain  $\Omega$  of volume  $V$ , the global (mean) dissipated energy  $\Delta$  is expressed as

$$\Delta = \frac{1}{V} \int_{\Omega} D(\Sigma_0^{\text{eq}}) dV \quad (6)$$

In the following, it is assumed that the temperature is uniform. This hypothesis will be discussed for the experimental application. The mean dissipation  $\Delta$  is then introduced in the following heat conduction equation

$$\dot{\Theta} + \frac{\Theta}{\tau_{\text{eq}}} = \frac{f_r \Delta}{\rho C} \quad (7)$$

where  $\tau_{\text{eq}}$  is a characteristic time depending on the heat transfer boundary conditions [11],  $\rho$  the mass density,  $C$  the specific heat,  $f_r$  the load frequency and  $\Theta$  the mean temperature. There is no need to add a thermoelastic term, which is vanishing over one cycle because only mean steady-state temperatures are sought. The mean (uniform) steady-state temperature  $\bar{\Theta}$  can then be calculated.

For proportional loadings,  $\Delta$  is simplified as

$$\Delta = \frac{4m V_0}{h(m+1)(m+2)} \frac{H_{m+2}(\Sigma_{0M}^{\text{eq}})^{m+2}}{V_0 S_0^m} = \frac{4m V_0}{h(m+1)(m+2)} \frac{(\Sigma_{\text{eff diss}})^{m+2}}{V_0 S_0^m} \quad (8)$$

where  $\Sigma_{0M}^{\text{eq}} = \max_{\Omega} (\Sigma_0^{\text{eq}})$ ,  $\Sigma_{\text{eff diss}}$  the effective dissipative stress and  $H_{m+2}$  the heterogeneity stress factor [10] given by

$$H_{m+2} = \frac{1}{V} \int_{\Omega} \left( \frac{\Sigma_0^{\text{eq}}}{\Sigma_{0M}^{\text{eq}}} \right)^{m+2} dV \quad (9)$$

For non-proportional loadings, it is no longer possible to simplify  $\Delta$  because of the expression of  $D(\Sigma_0^{\text{eq}})$ .  $\Delta$  is then calculated with the same hypotheses, but using a numerical integration software. However, it is possible to define a non-proportional loading factor

$$G_{m+2} = \Delta / \Delta_{0M} \quad (10)$$

where  $\Delta_{0M}$  is the mean dissipated energy for a proportional and uniform loading and a von Mises stress amplitude  $\Sigma_{0M}^{\text{eq}}$  defined by

$$\Delta_{0M} = \frac{4m V_0}{h(m+1)(m+2)} \frac{(\Sigma_{0M}^{\text{eq}})^{m+2}}{V_0 S_0^m} \quad (11)$$

It is thus possible to extend the concept of effective stress for non-proportional loading as follows

$$\Sigma_{\text{eff th}} = G_{m+2}^{1/(m+2)} \Sigma_{0M}^{\text{eq}} \quad (12)$$

where  $G_{m+2} = H_{m+2}$  for proportional loadings. The steady-state temperature  $\bar{\Theta}$  reads in any case

$$\bar{\Theta} = \eta \frac{m}{(m+1)(m+2)} \frac{(\Sigma_{\text{eff diss}})^{m+2}}{V_0 S_0^m} \quad (13)$$

with  $\eta = 4f_r \tau_{\text{eq}} / h\rho C$ . Equation (13) shows that the thermal behaviour depends only on three parameters and the effective dissipative stress. In the following section, the previous analysis is applied to and validated on a medium carbon steel C45 (SAE45).

### 3. Validation of tension–torsion results

#### 3.1. Experimental configuration

A tubular specimen with 2 flat sections per head [12] is used for tension–torsion loadings. The ratio thickness/mean radius of the gauge section is equal to 0.24 (external and internal radii are respectively  $R_e = 7$  mm and  $R_i = 5.5$  mm). All samples are machined from the same bar of medium carbon steel C45 (SAE45), which is, as far as elastic and thermal parameters are concerned, homogeneous and isotropic. Experiments are performed using a tension–torsion servohydraulic-testing machine. Differential temperature measurements are obtained by using 2 thermocouples, one in contact with the centre of the external surface of the gauge zone and the other on the grip of the actuator. At a loading frequency of 5 Hz, 3000 cycles are needed for each step to reach steady state conditions. The macroscopic stress tensor that depends on the radius  $r$ , is expressed as

$$\Sigma(r) = \begin{bmatrix} \Sigma_{11} & \Sigma_{12} & 0 \\ \Sigma_{12} & 0 & 0 \\ 0 & 0 & 0 \end{bmatrix}, \quad \text{with } \Sigma_{11} = \Sigma_{\max} \cos(2\pi f_r t) \text{ and } \Sigma_{12} = \tau_{\max} \frac{r}{R_e} \cos(2\pi f_r t + \delta) \quad (14)$$

where  $f_r$  is the loading frequency,  $\Sigma_{\max}$  and  $\tau_{\max}$  the tensile and shear stress amplitudes and  $\delta$  the phase difference between shear and normal stresses.

A pure tension and a pure torsion loading path are first performed on two different samples. On a third one, a non-proportional path, later called ‘out-of-phase’ is carried out, corresponding to a von Mises circle in the tension–torsion stress space for a point of the gauge section at mean radius. One must note that for other points, the loading path is still an ellipse, but with the major to minor axis ratio different from  $\tau_{\max}/\Sigma_{\max} = \sqrt{3}$ .

#### 3.2. Validation of the uniformity assumption of steady-state temperature

The heat transfer boundary conditions are a constant and uniform temperature on the interface sample/grip ( $\theta_{\text{grips}} = 0$ ) and a convection condition  $(\frac{\partial \theta}{\partial r}) \pm h_1 \theta = 0$  on respectively internal and external faces of the tube, where the value of the heat transfer coefficient  $h_1$  is taken from the literature [11]. Grips are considered to be ‘far’ from the gauge section, so that the steady-state temperature of the gauge section  $\bar{\theta}$  is considered as a simple function of the radius  $r$ . The heat equation to solve reads

$$\dot{\bar{\theta}} - \frac{k}{\rho C} \frac{\partial}{r \partial r} \left( r \frac{\partial \bar{\theta}}{\partial r} \right) = \frac{f_r \Delta(r)}{\rho C} \quad (15)$$

where  $k$  is the thermal conductivity. Figure 1 shows in pure torsion that  $\theta$  is nearly uniform (i.e., variation less than 0.02%) despite a high heterogeneity of dissipation, which is experimentally checked by measuring temperatures on both external and internal surfaces. The steady-state temperature is thus uniform and Eq. (13) applies.

#### 3.3. Evaluation of the effective dissipative stress

In proportional tension–torsion,  $G_{m+2}$  reads

$$G_{m+2} = \frac{2}{R_e^2 - R_i^2} \int_{R_i}^{R_e} \left( \frac{\sigma_{\max}^2 + 3(\frac{r \tau_{\max}}{R_e})^2}{\sigma_{\max}^2 + 3\tau_{\max}^2} \right)^{\frac{m+2}{2}} r \, dr \quad (16)$$

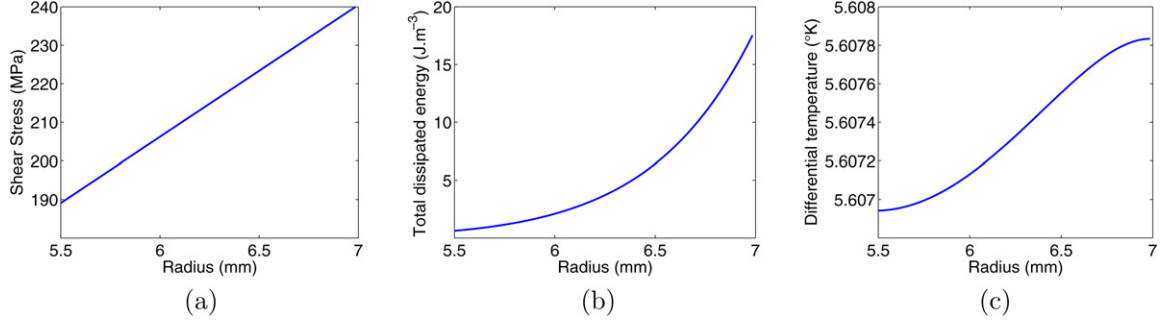


Fig. 1. Change of shear stress (a), total dissipated energy (b) and temperature (c) as functions of radius ( $k = 50 \text{ W m}^{-1} \text{ K}^{-1}$ ,  $\rho = 7900 \text{ kg m}^{-3}$ ,  $C = 500 \text{ J kg}^{-1} \text{ K}^{-1}$ ,  $\tau_{\text{eq}} = 70 \text{ s}$ ).

Fig. 1. Variation de la contrainte de cisaillement (a), de l'énergie dissipée totale (b) et de la température (c) en fonction du rayon ( $k = 50 \text{ W m}^{-1} \text{ K}^{-1}$ ,  $\rho = 7900 \text{ kg m}^{-3}$ ,  $C = 500 \text{ J kg}^{-1} \text{ K}^{-1}$ ,  $\tau_{\text{eq}} = 70 \text{ s}$ ).

Table 1

Values of  $H_{m+2}$  and  $G_{m+2}$  for different loading path when  $R_e = 7 \text{ mm}$ ,  $R_e = 5.5 \text{ mm}$ ,  $m = 12$

Tableau 1

Valeurs de  $H_{m+2}$  et  $G_{m+2}$  pour différents trajets de chargement dans le cas  $R_e = 7 \text{ mm}$ ,  $R_e = 5.5 \text{ mm}$ ,  $m = 12$

	Tension	Torsion	Heterogeneous out-of-phase	Uniform out-of-phase
$H_{m+2}$	1	0.32	0.36	1
$G_{m+2}$	1	0.32	7.29	7.24

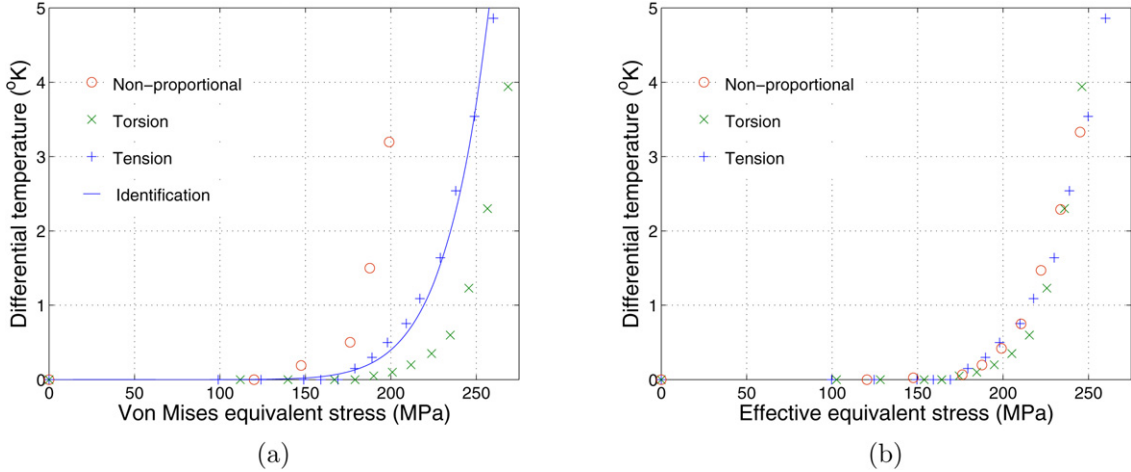


Fig. 2. Steady-state temperature for different loading paths: tension (+), torsion (x) and non-proportional (o) as functions of von Mises equivalent stress amplitude (a) and effective stress amplitude (b).

Fig. 2. Température stabilisée pour différents trajets de chargement (traction (+), torsion (x) et non-proportionnel (o)) tracée en fonction de la contrainte équivalente de von Mises de l'amplitude (a) et de la contrainte effective de l'amplitude (b).

and for the non-proportional loading,  $G_{m+2}$  is numerically calculated. As shown in Table 1 for the present geometry and material parameters, values of  $G_{m+2}$  for heterogeneous out-of-phase loading path (hypothesis of tension–torsion on thick-walled specimen) and uniform out-of-phase loading path (hypothesis of thin-walled specimen) influence the result. In the case of out-of-phase loading path, values of  $G_{m+2}$  greater than one are due to higher intrinsic dissipated energy than for proportional loading.

The experimental analysis consists in identifying the parameter  $m$  (e.g., using the steady-state temperature measurements in tension [2], see Fig. 2(a)) and then calculating the different heterogeneity factors to plot the other paths as shown in Fig. 2(b). To show the influence of the factor  $G_{m+2}$ , experimental results are directly plotted in Fig. 2(a) as

functions of von Mises equivalent stress amplitude. Figure 2(b) shows that the effective stress allows one to collapse all the experimental data onto a single curve.

#### **4. Summary**

Self-heating measurements under different proportional and non-proportional cyclic loadings have been performed in tension–torsion. Plotting results as functions of von Mises equivalent stress amplitude is not the adequate method (Fig. 2(a)). The stress heterogeneity effect induced by the probabilistic treatment of the experiments needs to be accounted for. Last, by using only one loading path result (e.g., tension) to identify the parameters, it is possible to calculate a heterogeneity factor that allows for the prediction of all other tested loading paths as shown in Fig. 2(b). The next step is the fatigue prediction under multiaxial loadings and its validation.

#### **References**

- [1] A. Galtier, O. Bouaziz, A. Lambert, Influence de la microstructure des aciers sur leurs propriétés mécaniques, *Méc. Ind.* 3 (2002) 457–462.
- [2] C. Doudard, S. Calloch, F. Hild, P. Cugy, A. Galtier, A probabilistic two-scale model for high cycle fatigue life predictions, *Fatigue Fract. Engrg. Mater. Struct.* 28 (2005) 279–288.
- [3] J.-C. Krapez, D. Pacou, C. Bertin, Application of lock-in thermography to rapid evaluation of fatigue limit in metals, in: Proceedings of the 5th AITA, Venezia (Italy), 1999.
- [4] G. La Rosa, A. Risitano, Thermographic methodology for rapid determination of the fatigue limit of materials and mechanical components, *Int. J. Fatigue* 22 (2000) 65–73.
- [5] E. Charkaluk, A. Constantinescu, Estimation of the mesoscopic thermoplastic dissipation in High-Cycle Fatigue, *C. R. Mecanique* 334 (2006) 373–379.
- [6] C. Doudard, S. Calloch, F. Hild, P. Cugy, A. Galtier, Identification of the scatter in high cycle fatigue from temperature measurements, *C. R. Mecanique* 332 (2004) 795–801.
- [7] C. Doudard, M. Poncelet, S. Calloch, C. Boue, F. Hild, A. Galtier, Determination of an HCF criterion by thermal measurements under biaxial cyclic loading, *Int. J. Fatigue* 29 (4) (2007) 748–757.
- [8] P. Cugy, A. Galtier, Microplasticity and temperature increase in low carbon steel, in: Proceedings of the 7th Int. Fat. Conf., Stockholm (Sweden), 2002.
- [9] M. Berveiller, A. Zaoui, An extension of the self-consistent scheme to plastically flowing polycrystals, *J. Mech. Phys. Solids* 26 (1979) 325–344.
- [10] F. Hild, R. Billardon, D. Marquis, Hétérogénéité des contraintes et rupture des matériaux fragiles, *C. R. Acad. Sci. Paris, II* 315 (1992) 1293–1298.
- [11] A. Chrysochoos, H. Louche, An infrared image processing to analyse the calorific effects accompanying strain localisation, *Int. J. Engrg. Sci.* 38 (2000) 1759–1788.
- [12] J. Lemaitre, J.-L. Chaboche, *Mécanique des matériaux solides*, Dunod, Paris, 1988, p. 90.